

Image restoration using the chiral Potts spin-glass

Domenico M. Carlucci

Instituut voor Theoretische Fysica,

K. U. Leuven, B-3001 Leuven, Belgium

Jun-ichi Inoue

Department of Physics, Tokyo Institute of Technology,

Oh-okayama, Meguro-ku, Tokyo 152-8551, Japan

(April 23, 2018)

Abstract

We report on the image reconstruction (IR) problem by making use of the random chiral q -state Potts model, whose Hamiltonian possesses the same gauge invariance as the usual Ising spin glass model. We show that the pixel representation by means of the Potts variables is suitable for the gray-scale level image which can not be represented by the Ising model. We find that the IR quality is highly improved by the presence of a glassy term, besides the usual ferromagnetic term under random external fields, as very recently pointed out by Nishimori and Wong. We give the exact solution of the infinite range model with $q = 3$, the three gray-scale level case. In order to check our analytical result and the efficiency of our model, 2D Monte Carlo simulations have been carried out on real-world pictures with three and eight gray-scale levels.

PACS numbers : 02.50.-r, 05.20.-y, 05.50.-q

INTRODUCTION

Recently, statistical mechanical approaches to the problems of information science attracted much attention of the researchers who are working in the field of information science. Among these, a particular interest has been given to the techniques by which one tries to reconstruct an image from its corrupted version, *e.g.* sent by a defective fax, a fickle *e-mail et cetera*, since any data transmission through a channel is in principle affected by some kind of noise. In the mathematical engineering fields, the traditional way to obtain the optimal recovered image has been regarded as a sort of optimization problems. In this framework, one first constructs the energy (cost) function so that this function represents the distance between the original image and the recovered one as properly as possible; then, one minimizes it using suitable heuristic methods like *simulated annealing* [1]. In fact, Geman and Geman [2] succeeded in constructing a method of image restoration using simulated annealing, and they discussed in detail the properties of its convergence including the optimal annealing schedule.

Successful results in this direction have been reached by means of the usual techniques of disordered spin systems, assuming that each spin is naturally associated to a pixel or bit. In the language of the disordered spin systems, the optimization problems we just mentioned are naturally translated into the search of the ground state a system possessing many local minima of order $\exp(N)$. In contrast, Marroquin *et al.* [3] found that the temperature of the system plays an important role for the image recovering process. From the statistical mechanical point of view, each recovered image can be regarded as the equilibrium state of a random spin systems. Marroquin *et al.* [3] investigated the effect of the temperature on the quality of image restoration by computer simulation and found the optimality of finite temperature image restoration. Recently, this finite temperature effects on image restoration was checked in a more careful way by Pryce and Bruce [4], although these works were restricted to numerical simulations. In the context

of the convolutional error-correcting codes, Ruján [5] proposed the finite temperature decoding in which we regard the sign of the local magnetization at a specific temperature (this temperature is well known as the *Nishimori temperature* [6] in the field of spin-glasses) as the correct bit. Recently Nishimori and Wong [7] pointed out that the optimal restoration of an image is also obtained at some specific temperature and showed that image restoration(IR) and error-correcting codes theory (ECC) can be treated within a single framework. Indeed, to the usual IR Hamiltonian, ferromagnetic and random field terms, they added a spin-glass term borrowed from the ECC theory [8] used for *parity-check*. They could exactly solve the infinite range spin model and find the optimal values of the temperature and the field (referred to as *hyper-parameters* from now on) at which the best retrieval quality is achieved. However, their works are restricted to the case of Ising spin systems and in this sense they are able to restore black/white pictures. On the other hand, there remain many open questions about the restoration of multi-color images or, somehow equivalently, gray toned images. This kind of problem has been also widely studied in the context of neural network with multi-state neurons, able to store and retrieve gray-scaled patterns (see [9] and references therein). For our purposes, we therefore map the set of the pixels onto q -state (chiral) Potts spins, with a ferromagnetic Hamiltonian in the presence of a random field (conventional IR) and, further on, a glass term (ECC-*like* term). The choice of the chiral Potts Hamiltonian is motivated by the fact that it exhibits the same gauge invariance as the Ising glass, although a work for the usual random Potts model is under consideration. Here, we show that, as in the Ising case [7], the presence of the glass term significantly increases the quality of the reconstructed image. We should mention that several remarkable studies about IR using the Potts model have been made by several authors. However, their works mostly depend on the computer simulations. In addition, their methods (mean field annealing [10], cluster algorithm [11,12], *etc.*) are devoted to the restorations at zero temperature. Therefore, it seems that there exist a lot of open questions about IR using the Potts model, especially,

about the performance of the finite temperature restoration.

In the next section, we will introduce our model within the image restoration theory and adopt the overlap as a measure of the restoration quality. In Sec. III, we will discuss the infinite range model and give the exact expression for the overlap as a function of the temperature and the external field, thus obtaining a relation between the temperature of source image and that of restoration temperature. We shall also see the improvement of the restoration quality by adding the glassy term. Finally, in Sec. IV, guided by the infinite range results, we will give explicit and realistic examples of image reconstructions for three and eight gray-scale picture.

I. THE MODEL AND IR FORMULATION

As already mentioned in Introduction, we choose to represent pixels of a gray-scaled image by means of q -component Potts spin variables. The usual Potts Hamiltonian $H = -\sum \delta_{\sigma_i \sigma_j}$ admits a complex representation [13] by means of the following identity

$$\delta_{\sigma_i \sigma_j} = \frac{1}{q} \sum_{r=0}^{q-1} (\sigma_i)^r (\sigma_j)^{q-r} \quad (1)$$

where each spin takes on one of the q roots of unity

$$\sigma_i = \exp\left(\frac{2\pi i}{q} K_i\right) \quad (K_i = 0, \dots, q-1). \quad (2)$$

From now on, we will use the notation $\{\xi\}$ for the original pixels and $\{\sigma\}$ for the variables of the recovering process. Let us now send the original image through a noise channel not only by the form of ξ_i^r itself but also by the following products $\xi_i^r \xi_j^{r*} = \xi_i^r \xi_j^{q-r}$. Without loss of generality we raised the spins and their products to some power r , since this corresponds only to a rotation in the complex circle. The reasons of this choice will be clear soon. For this expression, the output $(\{\tau^{(r)}\}, \{J^{(r)}\})$ is stochastically determined by the channel. For instance, in the case of a Gaussian channel (GC) the output function $P_{\text{out}}(\{J^{(r)}\}, \{\tau^{(r)}\}|\{\xi\})$ is given by

$$\begin{aligned}
P_{\text{out}}(\{J^{(r)}\}, \{\tau^{(r)}\}|\{\xi\}) &= \frac{1}{(2\pi J)^{N_B/2}} \frac{1}{(2\pi\tau)^{N/2}} \\
&\times \exp \left[-\frac{1}{2J^2} \sum_{(ij)} \sum_{r=0}^{q-1} (J_{ij}^{(r)} - J_0 \xi_i^r \xi_j^{q-r})(J_{ij}^{(r)*} - J_0 \xi_i^{q-r} \xi_j^r) \right] \\
&\times \exp \left[-\frac{1}{2\tau^2} \sum_i \sum_{r=0}^{q-1} (\tau_i^{(r)} - \tau_0 \xi_i^r)(\tau_i^{(r)*} - \tau_0 \xi_i^{q-r}) \right], \quad (3)
\end{aligned}$$

where $J_{ij}^{(r)}$ and $\tau_i^{(r)}$ are complex numbers which satisfy

$$(J_{ij}^{(r)})^* = J_{ij}^{(q-r)} \quad (\tau_i^{(r)})^* = \tau_i^{(q-r)} \quad (4)$$

in order to insure the realness of the sums in (3).

Obviously, if a noise-free transmission could be achieved, we would obtain $\tau_i^{(r)} = \xi_i^r$ and $J_{ij}^{(r)} = \xi_i^{q-r} \xi_j^r$. The conditional probability $P(\{\sigma\}|\{J^{(r)}\}, \{\tau^{(r)}\})$, which is probability that the source sequence is $\{\sigma\}$ provided that the outputs are $\{J\}$ and $\{\tau\}$, according to the Bayes theorem reads

$$P(\{\sigma\}|\{J^{(r)}\}, \{\tau^{(r)}\}) \sim \exp \left(\frac{\beta_J}{q} \sum_{(ij)} \sum_{r=1}^{q-1} J_{ij}^{(r)} \sigma_i^{(r)} \sigma_j^{(q-r)} + \frac{h}{q} \sum_i \sum_{r=1}^{q-1} \tau_i^{(r)} \sigma_j^{(q-r)} \right) P_d(\sigma) \quad (5)$$

where $P_d(\sigma)$ is a model of the prior distribution $P_s(\xi)$, that is,

$$P_d(\sigma) \equiv \exp \left(\frac{\beta_d}{q} \sum_{(ij)} \sum_{r=1}^{q-1} \sigma_i^{(r)} \sigma_j^{(q-r)} \right). \quad (6)$$

Our choice of the above prior distribution (6) is due to the assumption that in real world, images should be locally smooth. From this point of view, the distribution (6) is suitable because it gives high probability if the nearest neighboring sites take a same value.

For the Ising model, in order to get the restored pixels out of the average quantities, the pixel at site i (to be denoted as Σ_i) is naturally taken as the sign of the local magnetization. This means that the restored pixel is chosen as $\Sigma = +1$ ($\Sigma = -1$) if the spin points upward (downward) on average at the equilibrium. For our model, instead, since the value of the local magnetization is not simply confined to the interval $[-1, 1]$ but it runs all over the complex circle, we introduce the following generalized restored variable

$$\Sigma_i(\langle\sigma_i\rangle) = \exp \left[i \sum_{\alpha=0}^{q-1} \frac{2\pi}{q} \alpha \Xi_\alpha(\theta_i) \right] \quad (7)$$

with

$$\Xi_\alpha(x) = \Theta \left(x - \frac{2\pi}{q} \alpha + \frac{\pi}{q} \right) - \Theta \left(x - \frac{2\pi}{q} \alpha - \frac{\pi}{q} \right), \quad (8)$$

Θ being the usual step function, and

$$\theta_i = \tan^{-1} \left(\frac{\langle \text{Re} [\sigma_i] \rangle}{\langle \text{Im} [\sigma_i] \rangle} \right). \quad (9)$$

In simpler words, Σ_i is the closest spin on the circle to the value of the local magnetization $\langle\sigma_i\rangle \equiv \langle \text{Re} [\sigma_i] \rangle + i \langle \text{Im} [\sigma_i] \rangle$. For $q = 2$, it is straightforward to check that (7) reduces to a sign function up to a normalization constant. The quantities $\langle \text{Re} [\sigma_i] \rangle$ and $\langle \text{Im} [\sigma_i] \rangle$ are the average over the Boltzmann distribution $e^{-\mathcal{H}_{\text{eff}}}$ with the following effective Hamiltonian [14]

$$\mathcal{H}_{\text{eff}} - \frac{\beta_J}{q} \sum_{\langle ij \rangle} \sum_{r=1}^{q-1} J_{ij}^{(r)} (\sigma_i)^r (\sigma_j)^{q-r} - \frac{\beta_d}{q} \sum_i \sum_{r=1}^{q-1} (\sigma_i)^r (\sigma_i)^{q-r} - h \sum_i \sum_{r=1}^{q-1} \tau_i^{(r)} \sigma_i^{q-r}. \quad (10)$$

The condition (4) gives the above Hamiltonian the same spin gauge-symmetry as Ising spin glass, thus suppressing the spontaneous magnetization at low temperature which is present in the usual random Potts model. For the restoration purposes, the random field term aligns the spins according to the corrupted picture, whereas the ferromagnetic term insures the smoothness, by suppressing the isolated pixels within one small cluster. Therefore, a balance between β_d and h) will helps us to reconstruct the original picture well. The first term, instead, has been recently introduced in the problem of image restoration by Nishimori and Wong [7] and this term has been well known as the *parity check codes* in the field of error-correcting codes. Obviously, this term carries much more information about the original picture than the other two terms. Therefore, the performance of the image recovery is expected to be improved by this term. As a measure of the restoration quality, we shall adopt the following overlap M

$$M = \left[\frac{1}{q} \sum_{r=0}^{q-1} \xi_i^{q-r} \Sigma_i^r \right]_{\{\xi, J, \tau\}} \equiv \frac{1}{q} \sum_{r=0}^{q-1} \sum_{\xi} \sum_J \sum_{\tau} P_{\text{out}}(\{J^{(r)}\}, \{\tau^{(r)}\} | \{\xi\}) P(\xi) \xi_i^{q-r} \Sigma_i^r \quad (11)$$

in which $(1/q) \sum_{r=0}^{q-1} \xi_i^{q-r} \Sigma_i^r$ at each single site gives 1 if the original spin is in the same state as the restored one, and zero otherwise. Here the dependence on the local magnetization is buried in the angle θ_i , give by Eq. (9), and the sum over all the sites is understood. The main goal of this paper is to maximize the overlap M as a function of the temperatures (β_J and β_d) and the external field h (referred to as an estimate of the *hyper-parameters*). In the next section, we will start with an exactly solvable model, that is, an infinite range version of the Potts spin-glass.

II. MEAN FIELD SOLUTION

We will now investigate the performance of our model within the mean field approximation, *viz.* each spin is influenced by all the others. As the source image, we will consider a ferromagnetic state generated by a Boltzmann distribution at some finite temperature T_s . For the sake of simplicity, we will restrict ourselves to the case of $q = 3$, although the results can be generalized to any value of q . We thus assume that the original set of pixels $\{\xi\}$ is generated by a ferromagnetic 3-state Potts Hamiltonian with probability

$$P(\xi) = \frac{1}{\mathcal{Z}_s(\beta_s)} \exp \left[\frac{\beta_s}{2N} \sum_{i < j} (\xi_i \xi_j^* + \xi_i^* \xi_j) \right] \quad (12)$$

where $\mathcal{Z}_s(\beta_s)$ is a normalization constant and β_s is the inverse source temperature. According to the conditional probability, the observable are computed as

$$[\langle f \rangle]_{\{\xi, J, \tau\}} = \sum_{\xi} \sum_J \sum_{\tau} P(\{J^{(r)}\}, \{\tau^{(r)}\} | \{\xi\}) P(\xi) \frac{\text{Tr}_{\sigma} f e^{-\mathcal{H}_{\text{eff}}}}{\mathcal{Z}} \quad (13)$$

with

$$\mathcal{Z} \equiv \text{Tr}_{\sigma} \exp(-\mathcal{H}_{\text{eff}}). \quad (14)$$

It is rather straightforward to average out the disorder by means of the well-known replica trick [16] and, assuming replica symmetry ansatz and isotropy (no dependence on r), the saddle point equations for the order parameters are given by

$$[\langle \sigma_i^r \rangle] \equiv m = \frac{1}{\mathcal{Z}_s} \sum_{\xi} e^{\beta_s(m_s^{(1)} \text{Re}[\xi] + m_s^{(2)} \text{Im}[\xi])} \int \frac{du}{\sqrt{\pi}} \frac{dv}{\sqrt{\pi}} e^{-u^2 - v^2} \frac{Z_{\cos}(\xi)}{Z(\xi)} \quad (15)$$

$$[\text{Re}[\xi_i] \langle \sigma_i^r \rangle] \equiv t_1 = \frac{1}{\mathcal{Z}_s} \sum_{\xi} \text{Re}[\xi] e^{\beta_s(m_s^{(1)} \text{Re}[\xi] + m_s^{(2)} \text{Im}[\xi])} \int \frac{du}{\sqrt{\pi}} \frac{dv}{\sqrt{\pi}} e^{-u^2 - v^2} \frac{Z_{\cos}(\xi)}{Z(\xi)} \quad (16)$$

$$[\text{Im}[\xi_i] \langle \sigma_i^r \rangle] \equiv t_2 = \frac{1}{\mathcal{Z}_s} \sum_{\xi} \text{Im}[\xi] e^{\beta_s(m_s^{(1)} \text{Re}[\xi] + m_s^{(2)} \text{Im}[\xi])} \int \frac{du}{\sqrt{\pi}} \frac{dv}{\sqrt{\pi}} e^{-u^2 - v^2} \frac{Z_{\cos}(\xi)}{Z(\xi)} \quad (17)$$

$$\begin{aligned} [\langle \sigma_i^r \rangle \langle \sigma_j^{q-r} \rangle] \equiv Q &= \frac{1}{\mathcal{Z}_s} \sum_{\xi} e^{\beta_s(m_s^{(1)} \text{Re}[\xi] + m_s^{(2)} \text{Im}[\xi])} \\ &\times \int \frac{du}{\sqrt{\pi}} \frac{dv}{\sqrt{\pi}} e^{-u^2 - v^2} \frac{1}{Z^2(\xi)} [Z_{\cos}^2(\xi) + Z_{\sin}^2(\xi)] \end{aligned} \quad (18)$$

Here $m_s^{(1)}$ and $m_s^{(2)}$ are simply the real and imaginary components of the source magnetization, *viz* the usual non-random Potts model [13] mean field equations

$$[\text{Re}[\xi_i]] \equiv m_s^{(1)} = \frac{1}{\mathcal{Z}_s} \left(e^{\beta_s m_s^{(1)}} - e^{-\frac{1}{2} \beta_s m_s^{(1)}} \cosh \left[(\sqrt{3}/2) \beta_s m_s^{(2)} \right] \right) \quad (19)$$

$$[\text{Im}[\xi_i]] \equiv m_s^{(2)} = \frac{1}{\mathcal{Z}_s} \sqrt{3} e^{-\frac{1}{2} \beta_s m_s^{(1)}} \sinh \left[(\sqrt{3}/2) \beta_s m_s^{(2)} \right] \quad (20)$$

and

$$\mathcal{Z}_s = e^{\beta_s m_s^{(1)}} + 2e^{-\frac{1}{2} \beta_s m_s^{(1)}} \cosh \left[(\sqrt{3}/2) \beta_s m_s^{(2)} \right] \quad (21-a)$$

$$Z_{\cos}(\xi) = e^{U(\xi)} - e^{-\frac{1}{2} U(\xi)} \cosh V \quad (21-b)$$

$$Z_{\sin}(\xi) = \sqrt{3} e^{-\frac{1}{2} U(\xi)} \sinh V \quad (21-c)$$

$$Z(\xi) = e^{U(\xi)} + 2e^{-\frac{1}{2} U(\xi)} \cosh V \quad (21-d)$$

with

$$U = u \left[\frac{\beta_J^2 J^2}{q^2} Q + \tau^2 h^2 \right]^{\frac{1}{2}} + \frac{\beta_d}{q} m + \frac{\beta_J J_0}{q} [t_1 \text{Re}[\xi] + t_2 \text{Im}[\xi]] + \tau_0 h \text{Re}[\xi] \quad (22-a)$$

$$V = \frac{\sqrt{3}}{2} \frac{\beta_J J}{q} Q^{\frac{1}{2}} v. \quad (22-b)$$

Finally, the overlap M is expressed as the following weighted average

$$M = \frac{1}{\mathcal{Z}_s} \sum_{\xi} e^{\beta_s(m_s^{(1)} \text{Re}[\xi] + m_s^{(2)} \text{Im}[\xi])} \int_{\mathcal{S}(\xi)} \frac{du}{\sqrt{\pi}} \frac{dv}{\sqrt{\pi}} e^{-u^2 - v^2} \quad (23)$$

receiving contributions from the following $q = 3$ regions in the complex circle

$$\mathcal{S}(1) = \left\{ u, v \mid -\frac{\pi}{3} \leq \tan^{-1} \frac{Z_{\sin}}{Z_{\cos}} \leq \frac{\pi}{3} \cap Z_{\cos} > 0 \right\} \quad (24\text{-a})$$

$$\begin{aligned} \mathcal{S}(e^{\frac{2\pi i}{3}}) = & \left\{ u, v \mid \left(\frac{\pi}{3} \leq \tan^{-1} \frac{Z_{\sin}}{Z_{\cos}} \leq \frac{\pi}{2} \cap Z_{\cos} \geq 0, Z_{\sin} > 0 \right) \right. \\ & \left. \cup \left(-\frac{\pi}{2} \leq \tan^{-1} \frac{Z_{\sin}}{Z_{\cos}} \leq 0 \cap Z_{\cos} \leq 0, Z_{\sin} \geq 0 \right) \right\} \end{aligned} \quad (24\text{-b})$$

$$\begin{aligned} \mathcal{S}(e^{\frac{4\pi i}{3}}) = & \left\{ u, v \mid \left(\frac{\pi}{2} \leq \tan^{-1} \frac{Z_{\sin}}{Z_{\cos}} \leq -\frac{\pi}{3} \cap Z_{\cos} > 0, Z_{\sin} \geq 0 \right) \right. \\ & \left. \cup \left(0 \leq \tan^{-1} \frac{Z_{\sin}}{Z_{\cos}} \leq \frac{\pi}{2} \cap Z_{\cos} < 0, Z_{\sin} \leq 0 \right) \right\}. \end{aligned} \quad (24\text{-c})$$

We first assume that the exchange term is absent ($\beta_J = 0$) [15], that is no redundancy is fed into the channel. In this case, the saddle point equations (15-18) are drastically simplified and the overlap (23) simply reads

$$M = \frac{e^{\beta_s m_s}}{\mathcal{Z}_s} \text{Erf} \left[-\sqrt{2} \frac{\beta_d m + \tau_0 h}{\tau h} \right] + \frac{e^{-\frac{1}{2}}}{\mathcal{Z}_s} \left\{ 1 - \text{Erf} \left[-\sqrt{2} \frac{\beta_d m - \tau_0 h}{\tau h} \right] \right\} \quad (25)$$

with the magnetization given by

$$\begin{aligned} m = & \frac{e^{\beta_s m_s}}{\mathcal{Z}_s} \int \frac{du}{\sqrt{\pi}} e^{-u^2} \frac{1 - \exp[-\frac{3}{2}(u\tau h + \beta_d m/q + \tau_0 h)]}{1 + 2\exp[-\frac{3}{2}(u\tau h + \beta_d m/q + \tau_0 h)]} \\ & + \frac{2e^{-\frac{1}{2}\beta_s m_s}}{\mathcal{Z}_s} \int \frac{du}{\sqrt{\pi}} e^{-u^2} \frac{1 - \exp[-\frac{3}{2}(u\tau h + \beta_d m/q - \tau_0 h/2)]}{1 + 2\exp[-\frac{3}{2}(u\tau h + \beta_d m/q - \tau_0 h/2)]} \end{aligned} \quad (26)$$

where we defined $\text{Erf}(x) \equiv \int_x^\infty e^{-x^2} dx / \sqrt{\pi}$.

The problem is thus reduced to a one-dimensional model, corresponding to an Ising model in which the length of spin turns out to be $(+1, -1/2)$ instead of $(+1, -1)$. This is not surprising if one thinks that the fluctuations along the imaginary axis are governed only by the glassy term, meanwhile the magnetic field acts along the real direction. In Fig. 1, we plotted the overlap M as a function of T_d for the some values of h . It is

straightforward to check that the maximum value of the overlap M_{\max} does not depend on magnetic field h , since at the stationary point ($\partial M/\partial\beta_d = 0$) m is proportional to the magnetic field

$$\frac{1}{2}\beta_s m_s = \frac{1}{3}m\beta_d \frac{\tau_0}{\tau^2 h} + \frac{1}{4} \frac{\tau_0^2}{\tau^2}. \quad (27)$$

This feature holds also for the Ising case, although the stationary equation (27) is simpler

$$\beta_s m_s = m\beta_d \frac{\tau_0}{\tau^2 h}. \quad (28)$$

Expression (27) is thought to be valid only for the infinite range model, as confirmed in the next section by numerical results in $d = 2$.

Now we set the decoding temperature at the optimal value, that is $M(T_d^{\text{opt}}) \equiv M_{\max}$ and we switch the exchange interaction ($\beta_J \neq 0$) as depicted in Fig. 2. We notice that also a small amount of redundancy highly improves the value of the overlap M_{\max} which quickly increases and slowly decreases, after the peak, meanwhile the exchange term becomes dominant on the ferromagnetic one.

III. MONTE CARLO SIMULATIONS FOR REAL WORLD PICTURE

Although for the mere restoration aims it is not wise to smoothen two points far away from each other, we shall see that the infinite range model provides a useful guide for the more interesting case of real-world pictures, since the results remain qualitatively similar. We thus carried out Monte Carlo simulations for realistic pictures with short-range effective Hamiltonian. In this case, the ferromagnetic term will be concerned only with the points within the range of interaction and two points far away will not influence each other. It would be extremely interesting to study the restoration quality as a function of the interaction radius, but this goes beyond the aim of the present work and we limit ourselves to a first nearest-neighbors interaction Hamiltonian. Therefore let us consider a simple $q = 3$ gray scale level picture (upper left of Fig. 3), where each pixels has been

randomly flipped to another value with some probability, say $p = 0.15$ (upper right of Fig. 3). The curves shown in Fig.5 are the result of the restoration process without the glassy term, that is $\beta_J = 0$, at different values of the ratio $H = h/\beta_d$. Here the maximum value of the overlap is achieved around $H_{\max} \equiv h/\beta_d \sim 0.6$ and $T_d \sim 0.2$ and the corresponding restored image is drawn in the lower left of Fig. 3. Adding the glassy term at H_{\max} fixed improves drastically the value of the overlap and the quality of the restored image (lower right of Fig. 3), drawn at the peak of the Fig. 6. The same procedure is repeated in the presence of higher noise, $p = 0.30$, at the same H_{\max} and $\beta_{J;\max}$ and the results of the restoration are shown in Figs. 4. Finally, we applied the same algorithm to an eight gray-scale level picture with 20% and 30% of noise, upper images in Figs. 7 and 8. The results without exchange term are shown in Fig. 9. Once again we find a maximum for some values of T_d and H and the corresponding restored images are in Fig. 10.

IV. CONCLUSIONS

In this paper, we investigated the possibility of gray-scaled image restoration using chiral random Potts model. We exactly solved the infinite ranged version thus deriving the explicit expression of the overlap as a function of the estimates of the hyper-parameters h , β_d and β_J . In the absence of the glassy term, we obtained the exact relation between the restoration temperature β_d and the source temperature β_s which gives the maximum value of the overlap. This seems a highly non-trivial result because it is natural for us to assume that the best recovery of the image should be achieved for $\beta_d = \beta_s$, as it turns out to be true for the Ising case [7]. The Monte Carlo results on real pictures confirmed the expected high improvement due to the presence of the redundancy, *i.e.* the glassy term. However, so far, in our prescription to recover a corrupted image at the best restoration values, one is supposed to know the original data. In other words, the receiver has to meet the sender at least once to find the optimal restoration values. Only after that, the other receivers will be able to get an optimal restoration for the

same image, provided that the channels remain, at least qualitatively, unchanged. In this sense, it would be extremely useful to provide some *a priori* criteria (the receiver will not be supposed to meet the sender) for the optimum values of the hyper-parameters, once that some intrinsic characteristics (*e.g.* temperature) of the original image are known. Therefore, in order to check if the relation (27) still holds down to two dimensions, we restored $q = 3$ ferromagnetic snapshots generated at some known temperature. However, so far we have not yet obtained reliable results and detailed investigations in this direction will be reported in a forth coming paper.

ACKNOWLEDGEMENT

We thank Prof. Hidetoshi Nishimori for useful discussions and showing us his paper prior to publication. We also thank Prof. Kazuyuki Tanaka for useful advice and fruitful discussions.

The authors were supported by JSPS-Royal Society/British Council Anglo-Japanese Scientific Cooperation Programme. One of the authors (D.M.C.) started this work under JSPS grant No.P96215.

REFERENCES

- [1] S. Kirkpatrick, C. D. Gelatt and M. P. Vecchi, *Science* **220**, 671 (1983).
- [2] S. Geman and D. Geman, *IEEE Trans. on Pattern Anal. Mach. Intel.* **6**, 721 (1984).
- [3] J. Marroquin, S. Mitter and T. Poggio, *J. American Stat. Assoc.* **82**, 76 (1987).
- [4] J. M. Pryce and A. D. Bruce, *J. Phys. A: Math. Gen.* **28**, 511 (1995).
- [5] P. Ruján, *Phys. Rev. Lett.* **70**, 2968 (1993).
- [6] H. Nishimori, *Prog. Theor. Phys.* **66**, 1169 (1981).
- [7] H. Nishimori and K. Y. M. Wong, *unpublished*.
- [8] N. Surlas, *Nature* **339**, 693(1989).
- [9] D. Bollé, B. Vinck and V. A. Zagrebnoy, *J. Stat. Phys.* **70**, 1099 (1993).
- [10] J. Zhang, *IEEE Trans. Signal Process.* **40**, 2570 (1992).
- [11] K. Tanaka and T. Morita, “ Theory and Applications of the Cluster Varidation and Path Probability Methods”, Edited by J. L. Morán-López and J. M. Sanches, Plenum Press, New York 1996.
- [12] T. Morita and K. Tanaka, *Pattern Recognition Letters* **18**, 1479 (1997).
- [13] L. Mittag and M. J. Stephen, *J. Phys. A* **7**, L109 (1974).
- [14] H. Nishimori and M. J. Stephen, *Phys. Rev. B* **27**, 5644 (1983).
- [15] H. Nishimori, *Phys. Rev. B* **28**, 4011 (1983).
- [16] D. Sherrington and S. Kirkpatrick, *Phys. Rev. Lett.* **35**, 1792 (1975).

FIGURES

FIG. 1. Overlap M as a function of T_d for different values of h . The maximum value M_{\max} does not depend on h .

FIG. 2. Overlap M_{\max} as a function of the exchange temperature β_J for several values of J_0 . The overlap improves even for small values of the exchange term.

FIG. 3. Upper left: original three gray-scale levels image. Upper right: 15% of noise. Lower left: restoration without exchange term. Lower right: restoration with exchange term.

FIG. 4. Upper left: original three gray-scale levels image. Upper right: 30% of noise. Lower left: restoration without exchange term. Lower right: restoration with exchange term.

FIG. 5. Overlap M as a function of the decoding temperature T_d at $\beta_J = 0$ (left). The system size is 64×72 and each line is averaged over different 4 samples.

FIG. 6. Overlap as a function of β_J . We set the parameters $(H, T_d) = (0.6, 0.2)$ which gives the maximum in the absence of the exchange term.

FIG. 7. Upper left: original eight gray-scale levels image. Upper right: 20% of noise. Lower left: restoration without exchange term. Lower right: restoration with exchange term.

FIG. 8. Upper left: original eight gray-scale levels image. Upper right: 30% of noise. Lower left: restoration without exchange term. Lower right: restoration with exchange term.

FIG. 9. Overlap M as a function of the decoding temperature T_d at $\beta_J = 0$ (left). The system size is 93×100 and each line is averaged over different 4 samples.

FIG. 10. Overlap as a function of β_J . We set the parameters $(H, T_d) = (0.6, 0.1)$ which gives the maximum in the absence of the exchange term.

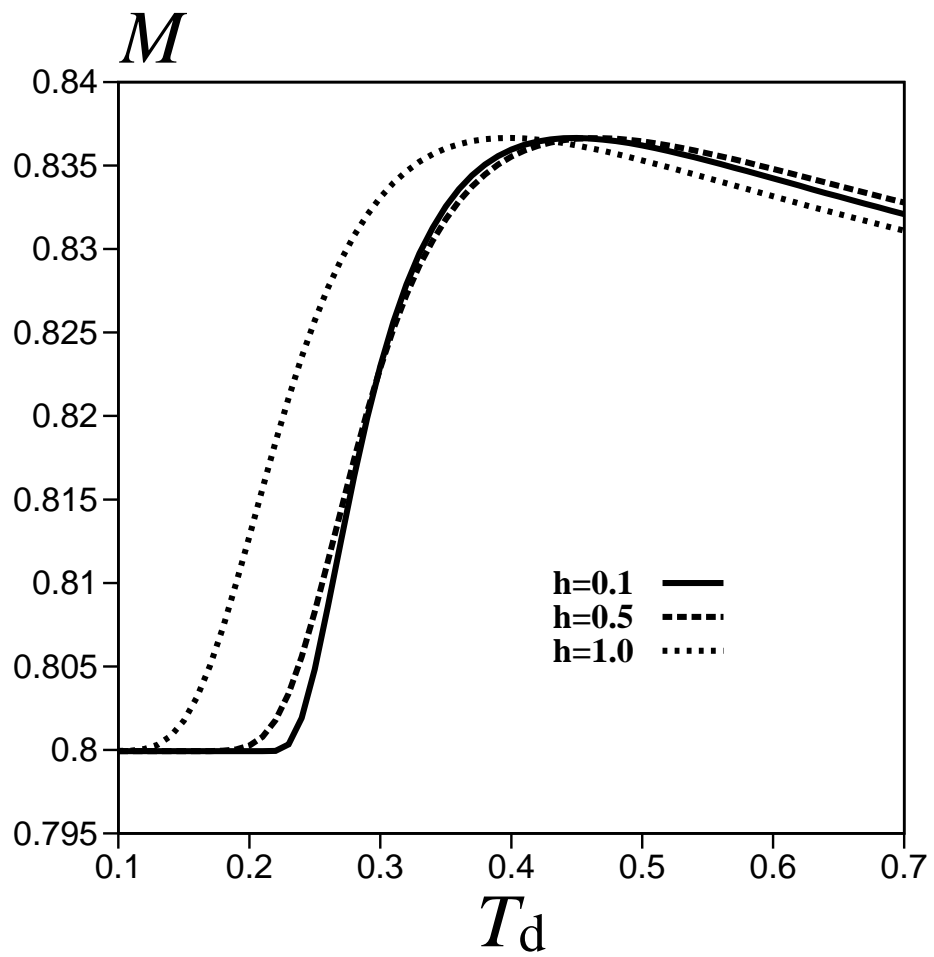


Fig. 1

D. M. Carlucci and J. Inoue

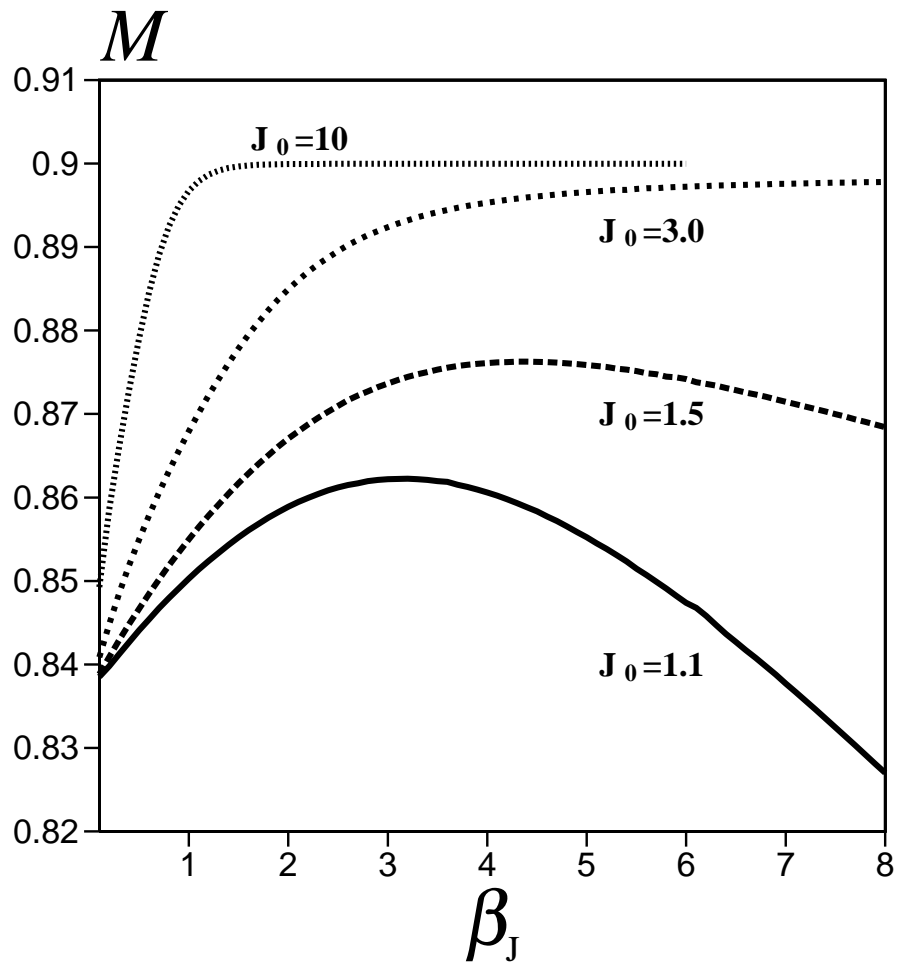


Fig. 2

D. M. Carlucci and J. Inoue

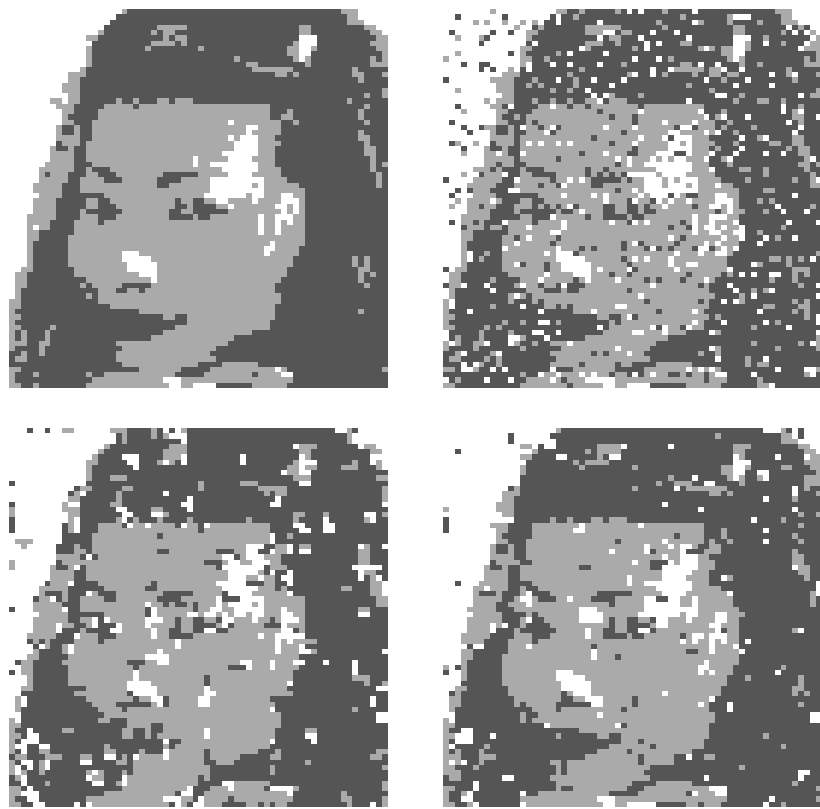


Fig. 3

D. M. Carlucci and J. Inoue

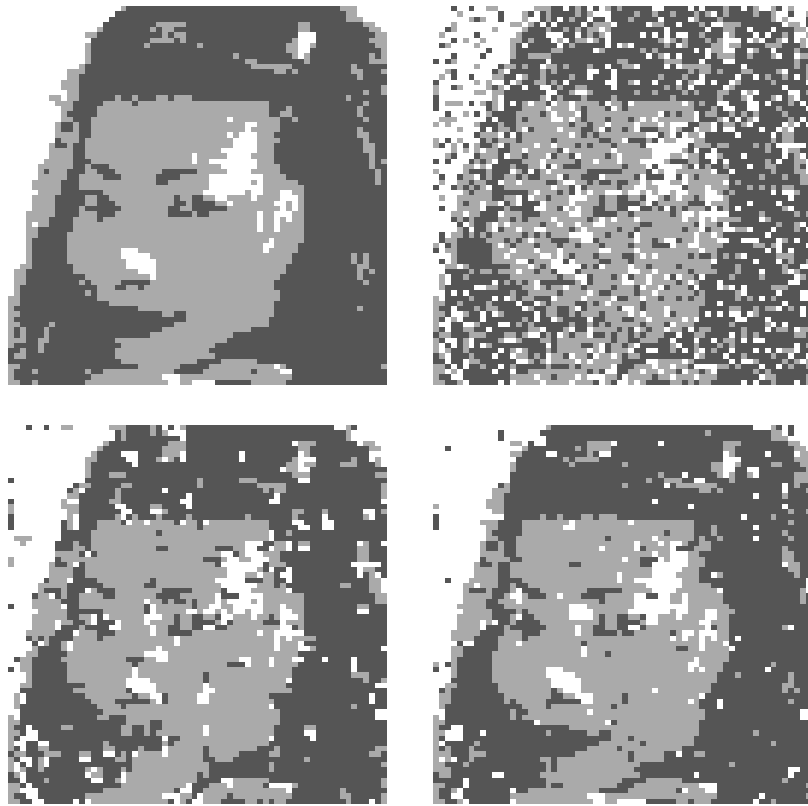


Fig. 4

D. M. Carlucci and J. Inoue

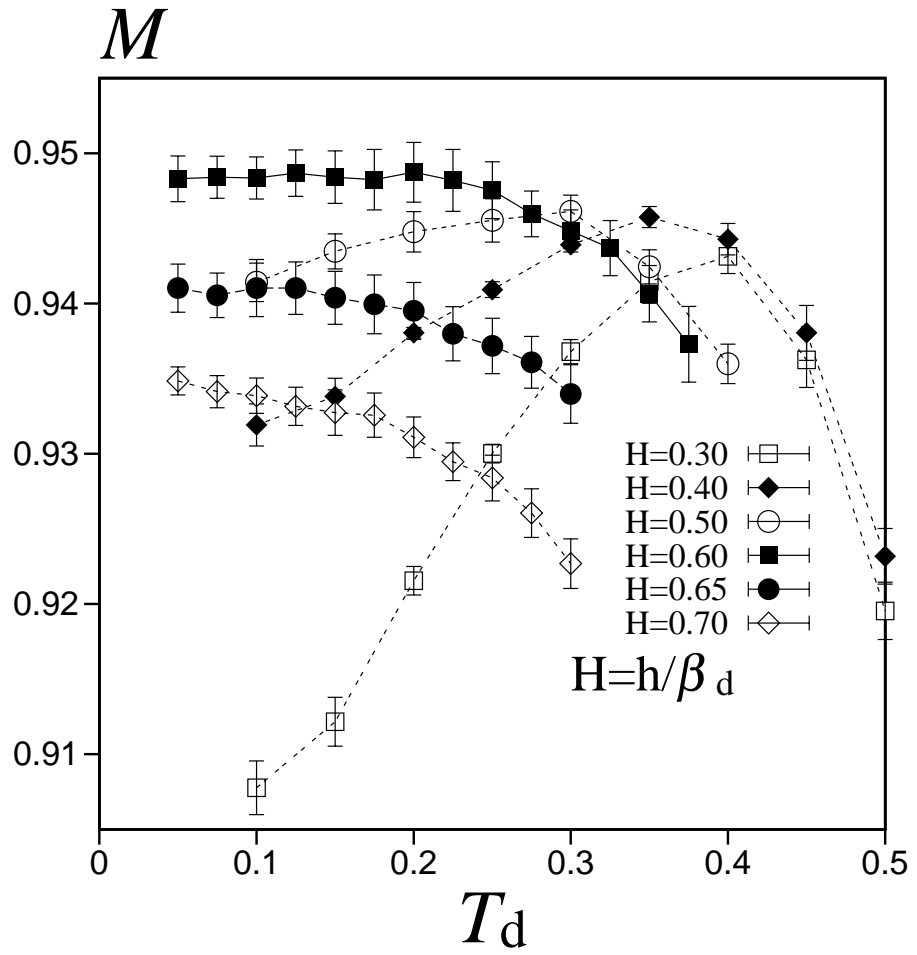


Fig. 5

D. M. Carlucci and J. Inoue

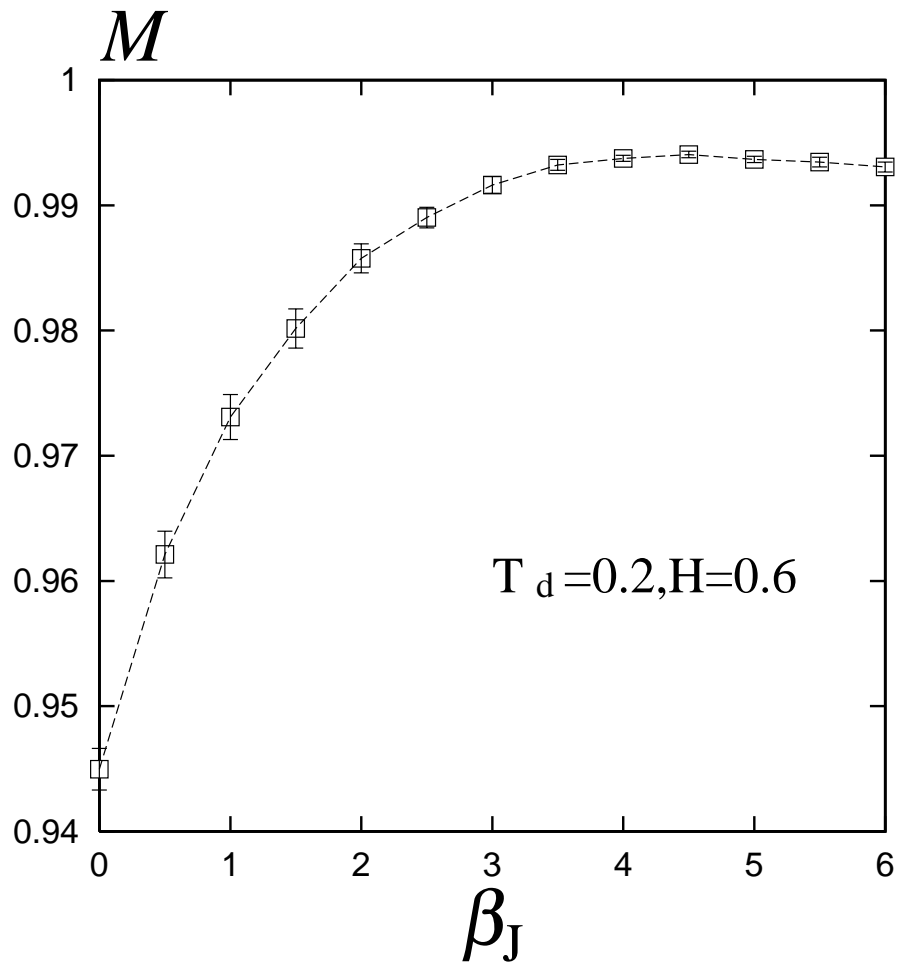


Fig. 6

D. M. Carlucci and J. Inoue



Fig. 7

D. M. Carlucci and J. Inoue

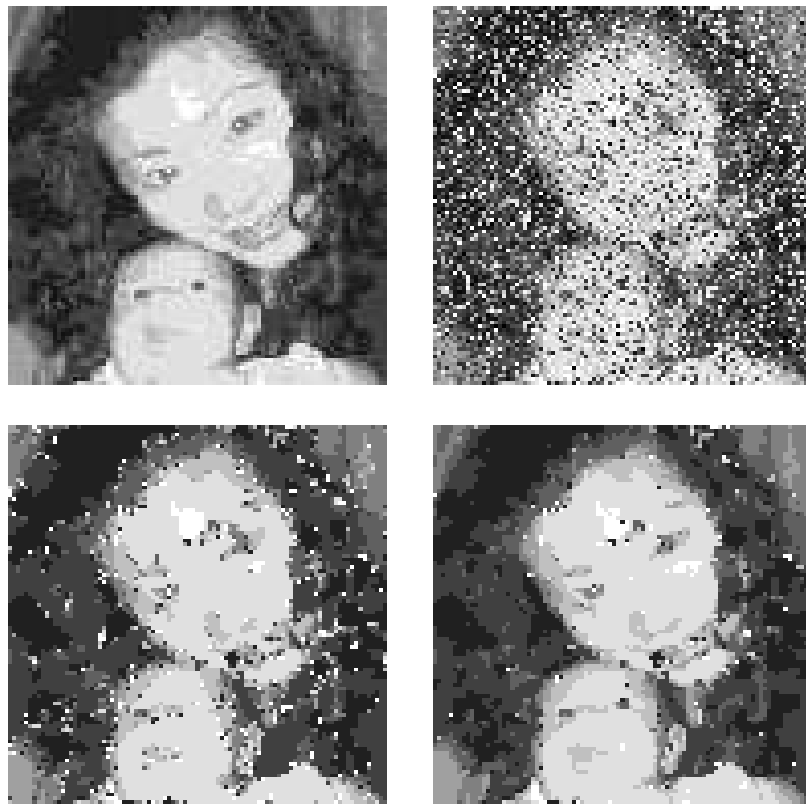


Fig. 8

D. M. Carlucci and J. Inoue

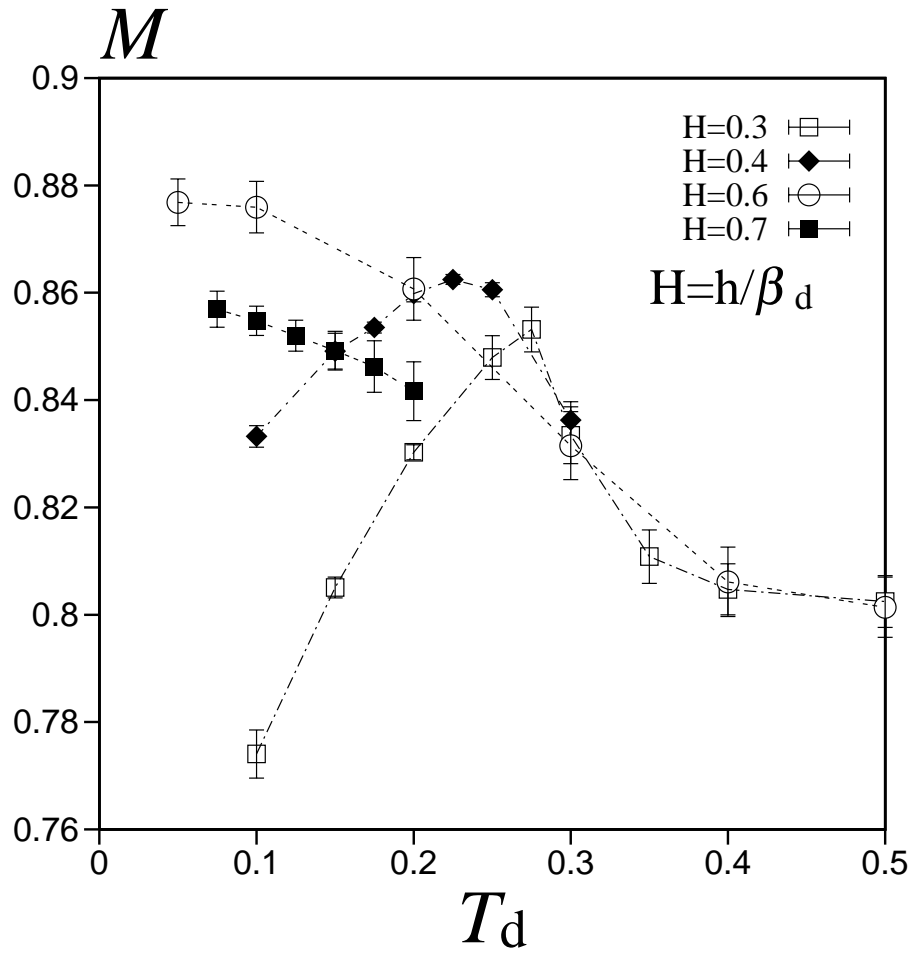


Fig. 9

D. M. Carlucci and J. Inoue

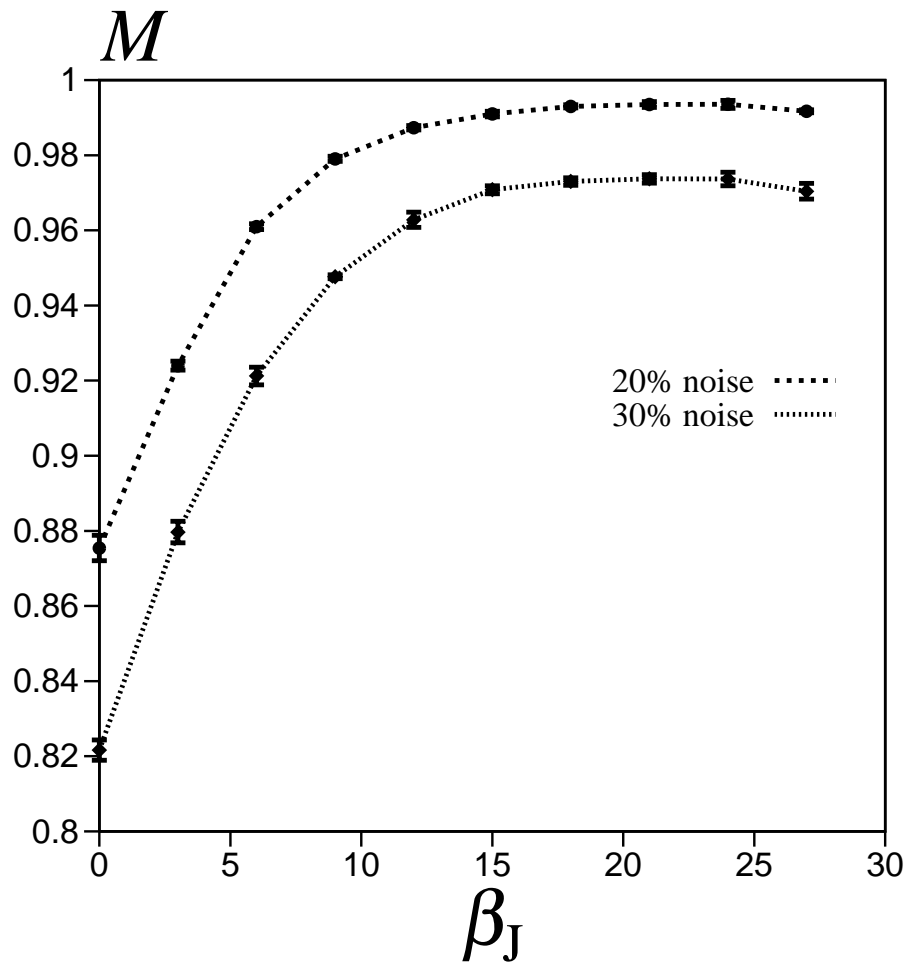


Fig. 10

D. M. Carlucci and J. Inoue